Neoplasma 2022; 69(4): 794–806

doi:10.4149/neo_2022_211002N1401

Methylation-mediated expression of SPARC is correlated with tumor progression and poor prognosis of breast cancer

Xiao-Long LI[1,2], Jia-Li LI[3], Dong-Jie QIU[4], Li MA[1,*]

[1]Breast Center, The Fourth Hospital of Hebei Medical University, Shijiazhuang, Hebei, China; [2]Department of Breast Surgery, The Fourth Hospital of Shijiazhuang, Shijiazhuang, Hebei, China; [3]Research Center, The Fourth Hospital of Hebei Medical University, Shijiazhuang, Hebei, China; [4]Department of Anesthesiology, The Fourth Hospital of Hebei Medical University, Shijiazhuang, Hebei, China

**Correspondence: malilaoshi2019@126.com*

Received October 10, 2021 / Accepted March 22, 2022

Secreted protein acidic and rich in cysteine (SPARC) plays a crucial role in the formation and progression of tumors. DNA methylation has become increasingly recognized as a frequent event of epigenetic alterations and one of the primary mechanisms of gene inactivation. The study aims to investigate the status of DNA methylation and the biofunction of SPARC in breast cancer. The qRT-PCR, BGS, and MSP methods were respectively employed to measure the relative mRNA expression levels and methylation status of SPARC. Additionally, the effects of SPARC on cell proliferation, migration, and invasion were examined in SPARC overexpression and knockdown cells. Immunohistochemical staining and western blot assay were used to examine the protein expression of genes. The expression levels of SPARC were found to be higher in breast cancer tissues and most breast cancer cells. The expression levels of SPARC in MDA-MB-231 and MCF-7 cells were significantly reversed by 5-Aza-dC treatment. Furthermore, the high expression and promoter DNA hypomethylation of SPARC were detected in triple-negative breast cancer tissues, while no expression changes of SPARC were found in luminal A breast cancer tissues. Overexpression of SPARC dramatically promoted MCF-7 cells migration and invasion, while knockdown of SPARC inhibited MDA-MB-231 cells migration and invasion. SPARC was involved in the epithelial-mesenchymal transition (EMT) process of breast cancer cells. The expression levels of mesenchymal markers N-cadherin, Vimentin, and β-catenin were upregulated, while E-cadherin was downregulated in SPARC overexpressed breast cancer cells. Conversely, the expression levels of EMT-related genes demonstrated the opposite trend in SPARC knockdown cells. To conclude, high expression of SPARC regulated by promoter hypomethylation promotes breast cancer cells migration and invasion, thus SPARC may act as an oncogene and serve as a potential target for breast cancer therapy.

Key words: secreted protein acidic and rich in cysteine (SPARC), DNA methylation, breast cancer, epithelial-mesenchymal transition (EMT)

Breast cancer (BC) is a malignant tumor that seriously threatens women's health [1] and it has now surpassed lung cancer as the leading cause of global cancer incidence in 2020, with an estimated 2.3 million new cases, representing 11.7% of all cancer cases. It is the fifth leading cause of cancer mortality worldwide, with 685,000 deaths [2]. It is imperative to identify effective diagnostic or prognostic molecular biomarkers for decreasing the recurrence and metastasis, and eventually reducing the mortality of BC.

Secreted protein acidic and rich in cysteine (SPARC, alternative names osteonectin; ON or basement-membrane-40; BM40) is an albumin-binding glycoprotein [3]. Previous studies have reported the poor prognostic role of SPARC in a number of aggressive cancers such as melanoma, glioma, colorectal cancer, and head and neck cancers [4–9]. SPARC was also reported to act as the inhibitory molecular in tumorigenesis in several types of human cancers, including ovarian cancer, prostate cancer, and pancreatic cancer [10–12]. SPARC was reported to be highly expressed in BC. More significantly, triple-negative breast cancer (TNBC), characterized by a high recurrence rate and high frequency of metastasis has a higher expression frequency of SPARC [3]. It was reported that SPARC regulated the activation of matrix metalloproteinase 2 (MMP-2) at the cell surface and contributed to the proteolytic pathways associated with breast cancer invasion [13]. SPARC can be a new biomarker helpful to identify more aggressive ductal carcinoma in situ (DCIS) and for the prediction of invasive disease on final pathology [14]. However, there were also some studies supporting the contrary effect. It was reported that high endogenous expres-

sion of SPARC in breast cancer cells reduced metastasis via decreasing invasive activity and tumor cell-platelet aggregation [15]. The distinct contribution of SPARC in BC needs to be further elucidated.

DNA methylation driven by DNA methyltransferases (DNMTs) has become increasingly recognized as a frequent event of epigenetic alterations and one of the primary mechanisms of gene dysfunction. Identifying reliable DNA methylation biomarkers not only can discover new indicators for screening and diagnosing cancer earlier, but also has the potential to be a strong prognostic factor. Aberrant DNA methylation of SPARC has been observed in several gastrointestinal malignancies including pancreatic and colorectal cancer [16]. The methylation pattern of SPARC was strongly associated with glioma-specific molecular alterations and may be helpful in monitoring glioma tumor progression and prognosis [17]. The promoter of SPARC was methylated in 68% of primary ovarian tumors and the protein expression levels of SPARC decreased as the disease progresses from low to high grade [18]. However, studies with rigorous methodology are needed to determine the spatial distribution of DNA hypomethylation and identify differentially methylated sites of SPARC associated with the risk of breast cancer [19]. Moreover, robust evidence of a prospective relationship between DNA methylation patterns and breast cancer risk remains to be further studied. In the present study, we detected the expression pattern of SPARC in BC, investigated the promoter methylation status of SPARC in the different molecular subtypes and the correlation of SPARC with malignant progression, and further detected the functional roles of SPARC in BC tumorigenesis.

Patients and methods

Patients and specimens. A total of 120 pairs of BC tissues and normal tissues were collected from patients that underwent surgery between September 2010 and September 2011 at the Fourth Hospital of Hebei Medical University. BC patients were divided into four molecular subtypes including luminal A, luminal B, HER-2 (+), and triple-negative breast cancer (TNBC), and there were 30 patients per subtype. The study was approved by the Ethics Committee of the Fourth Hospital of Hebei Medical University and conformed to all relevant ethical regulations for human research subjects in accordance with the Declaration of Helsinki. All the participants signed a written informed consent form. All these patients were females, with a median age of 48 years, and did not receive neoadjuvant chemotherapy and radiotherapy. All patients were continually followed after surgery and the follow-up deadline was September 1, 2021. Ninety (75.0%) patients survived, thirteen (10.8%) died of BC, three (2.5%) deaths were unrelated to BC, and fourteen (11.7%) patients were missing till the follow-up deadline. Freshly removed BC and paired adjacent normal tissues were divided into two groups, one of which was frozen and stored at –80 °C for DNA, RNA, and protein isolation, and the other was fixed in formalin at room temperature and embedded in paraffin for immunohistochemical (IHC) staining assay.

Cell culture and treatment. A total of 6 human cell lines (MCF-10A, MCF-7, MDA-MB-453, SK-BR-3, MDA-MB-549, and MDA-MB-231) were purchased from Procell (Procell, China). The MCF-7 cell line was cultured in RPMI-1640 medium (Gibco, USA). The cell lines (MDA-MB-453, SK-BR-3, MDA-MB-549, and MDA-MB-231) were cultured in a DMEM medium (Gibco, USA). The cell lines were supplemented with 10% fetal bovine serum (FBS; BI, Israel) at 37 °C in a humidified atmosphere of 5% CO_2. Human normal breast epithelial cell line MCF-10A was cultured according to the manufacturer's instructions (DMEM/F12 + 5% HS+20 ng/ml EG + 0.5 μg/ml hydrocortisone + 10 μg/ml insulin + 1% NEAA + 1% P/S (PB180120). Six cell lines (1.5×10^5/ml) were treated with 5 μM DNA methyltransferase inhibitor 5-aza-2'-deoxycytidine (5-Aza-dC; Sigma, Germany) with 10% FBS for 72 h with 5-Aza-dC changed every 24 h. Control cells received no drug treatment. DNA, RNA, and protein were isolated from these cells.

Quantitative real time reverse transcription polymerase chain reaction (qRT-PCR) analysis. Total RNA was extracted from tissue specimens and six cell lines using the Animal Total RNA Isolation Kit (Generay, China). The RT-for-PCR kit was used to synthesize single-stranded cDNA according to the manufacturer's protocol. The mRNA expression levels were quantified using primers, cDNA template, and Go Taq®qPCR MasterMix (Promega, USA), according to the protocol of Go Taq®qPCR Master Mix. The data were analyzed by the $2^{-\Delta\Delta}$Ct method and the human GAPDH gene was used as an endogenous control. Primer sequences and annealing temperature are listed in Supplementary Table S1.

Immunohistochemical staining assay. Protein expression of SPARC was detected by immunostaining using the avidin-biotin complex immunoperoxidase method, which was performed on the paraffin-embedded tumor tissue section and corresponding normal tissue section. Rabbit anti-human monoclonal antibody for SPARC (1:400, ab225716, Abcam, UK) was used to detect the protein expression of SPARC. Scoring accounted for both representation of the areas and the intensities of the stains [3]. All of the slides were examined concurrently by three experienced pathologists, who were blinded to the clinical data.

Western blot (WB) analysis. Tissue lysates were lysed in the radioimmunoprecipitation assay buffer (RIPA) with phenylmethanesulfonyl fluoride (PMSF; Solarbio, China). Total cellular proteins were harvested from cancer cell lines. The protein concentration of cell lysates was determined by the Pierce BCA Protein Assay kit (MultiSciences, China) according to the manufacturer's instructions. Equal amounts (30 μg) of cell lysates were separated by 12% SDS-PAGE and transferred onto a polyvinylidene difluoride membrane (Bio-Rad, USA). The membranes were blocked

and probed with the following primary antibodies overnight at 4 °C. The primary antibodies: E-cadherin (1:1000, 20874-1-AP, Proteintech, China), N-cadherin (1:1000, 22018-1-AP, Proteintech, China), Vimentin (1:1000, 10366-1-AP, Proteintech, China), β-catenin (1:1000, 20536-1-AP, Proteintech, China), SPARC (1:400, ab225716, Abcam, UK), and β-actin (1:1000, AF0003, Beyotime, China). Following washing with TBS-Tween-20, the membranes were incubated with peroxidase-conjugated affinipure secondary antibodies for 1 h at 37 °C. ImageJ software (National Institutes of Health, Bethesda, MD, USA) was employed to quantify protein levels.

DNA extraction and sodium bisulfite treatment. Genomic DNA was isolated from breast cancer cell lines, frozen BC tumor specimens, and corresponding normal tissues using a DNA extraction kit (Tiangen, China). To assess the DNA methylation patterns, DNA was bisulfite-modified using the DNA Bisulfite Conversion kit (Tiangen, China), which converts unmethylated cytosine residues to thymine, whereas methylated cytosine residues remain unaffected.

Methylated CpG site distribution via bisulfite genomic sequencing (BGS) and bisulfite conversion-specific and methylation-specific polymerase chain reaction (BS-MSP) assay. To analyze the DNA methylation pattern of SPARC, the BGS assay was first used to detect the methylated CpG sites distribution in breast cancer cell lines. The online MethPrimer program was used to detect the distribution of CpG islands. A pair of primers were designed by Sangon Biotech Co., Ltd. (Sangon, China) to recognize sodium bisulfite-converted genomic DNA (from −166 to +254 bp). The PCR products were purified using the QIAEXII Gel Extraction kit and cloned in top GEM-T easy vectors (Promega, USA). Up to 10 clones for each specimen were analyzed by bisulfite sequencing. According to the distribution of methylated CpG sites detected by BGS analyses, the methylation status of SPARC (from −8 to +133 bp) was then determined via BS-MSP assay using bisulfite-treated genomic DNA. The MSP primers were designed by Sangon Biotech Co., Ltd., and the reaction conditions are summarized in Supplementary Table S2. The BS-MSP products were analyzed on 2% agarose gel with ethidium bromide staining.

Cell transfection. For overexpression of SPARC, the cDNA encoding it was PCR-amplified and subcloned into pEZ-M98-vector (iGene Biotechnology Co., Ltd., China). FuGENE®6 Transfection Reagent (Promega, China) was used for cell transfection. According to the manufacturer's instructions, MCF-7 and MDA-MB-231 cells in the logarithmic growth phase were cultured in 6-well plates. When the density of cells reached 50–70%, 2 μg pEZ-M98-SPARC or pEZ-M98-NC was added to each well of a 6-well plate. For downregulation of SPARC, MCF-7 and MDA-MB-231 cells were transfected with siRNAs specific for SPARC (RiboBio, China). 50 nM siRNA-SPARC or siRNA-NC together with 12 μl transfection reagent (iGene China) and 10% FBS were added to each well of a 6-well plate for 24 h. Following transfection, the cells were incubated in DMEM/RPMI-1640 medium containing 10% FBS for 24 h. After that, the transfected cells were extracted for the subsequent experiment.

Cell proliferation assay. MCF-7 and MDA-MB-231 cells (4.0×10^3) following transfection for 24 h were seeded into 96-well plates for the cell proliferation assay. The proliferation of MCF-7 and MDA-MB-231 cells was determined by Cell Counting Kit-8 (CCK8; Promega, USA) at 0 h, 24 h, 48 h, 72 h, and 96 h following cell seeding. The absorbance was measured at a wavelength of 560 nm after incubation for 2 h in a humidified incubator containing 5% CO_2 at 37 °C. All the experiments were performed in triplicate.

Colony formation assay. For the colony formation assay, MCF-7 cells (2×10^3) following transfection for 24 h were seeded in 6-well plates and incubated with RPMI-1640 medium containing 10 % FBS for 14 days. MDA-MB-231 cells (2×10^3) following transfection for 24 h were seeded on 6-well plates with DMEM medium containing 10% FBS for 10 days. Colonies (>50 cells) were fixed in paraformaldehyde for 20 min (at room temperature) and stained with crystal violet dye (0.1 % w/v) for 30 min at room temperature, and the colony number was counted under an inverted microscope.

Wound healing assay. A wound was produced by a straight scratch with a 10 μl pipette tip in the cultured cells, and then the images were captured at the same position of each well 0 h and 48 h after the wound was created under a microscope. The relative distance of cell migration to the scratched area was measured and a healing percentage was calculated. The experiments were repeated in triplicate.

Transwell migration and invasion assays. Cell migration and invasion ability were investigated by Transwell assay. MCF-7 or MDA-MB-231 cells (4×10^4) following transfection were suspended in 200 μl DMEM or RPMI-1640 medium without FBS and seeded in the upper chambers (Corning, USA). A total of 600 μl DMEM/RPMI-1640 medium with 10% FBS was added to the lower chambers. The chambers were then cultured at 37 °C with 5% CO_2 for 24 h. For invasion assays, Transwell chambers coated with matrigel (BD Biosciences, USA) were used. Cells in the upper chamber were then carefully removed, while the cells in the lower chamber were stained with crystal violet dye (0.1% w/v) at 37 °C for 30 min. Cells were subsequently counted using a light microscope (magnification, ×100) and five random fields of view were selected to calculate cell numbers.

Statistical analysis. Statistical analysis was performed with SPSS 22.0 software package (Chicago, IL, USA). The qRT-PCR results were presented as the mean ± SD. Student's t-test was applied to compare the expression means between different continuous variables and one/two-way ANOVA was applied for multiple comparisons. All statistical tests were two-sided and $p<0.05$ was considered to indicate a statistically significant difference.

Results

The expression status of SPARC in BC tissues and breast cancer cell lines. The location of the SPARC genome from UCSC is shown in Figure 1A. The mRNA expression level of SPARC in human BC tissues was higher than that in normal breast tissues in TCGA database (Figure 1B). The mRNA expression levels of SPARC in 120 tumor specimens were significantly higher than that in corresponding normal tissues (Figure 1C). When analyzed according to molecular subtypes, the mRNA expression levels of SPARC in most subtype tumor tissues were higher than that in corresponding adjacent normal tissues, while no mRNA expression changes of SPARC were found in luminal A/B breast cancer tissues (Figure 1D). The protein expression of SPARC was further detected by IHC staining in tumor tissues and corresponding normal tissues (Figure 1E). The protein expression of SPARC in tumor tissues (35.0%, 42/120) was markedly increased compared with that in normal tissues (15.0%, 18/120; $p<0.05$; Table 1). When stratified by molecular subtype of BC, protein expression of SPARC was identified to be associated with molecular subtype and lymph node metastasis ($p<0.05$; Table 2). Then we detected the mRNA expression levels of SPARC in five BC cell lines and one human normal breast epithelial cell line MCF-10A, and we found that mRNA expression levels of SPARC in most BC cell lines were higher than that in normal breast epithelial cell line, except for MCF-7 cell line (Figure 1F). The protein expression of SPARC in BC cell lines and MCF-10A cells was further assessed by WB assay and the results were similar to those of mRNA expression (Figure 1G). The survival analysis showed that positive protein expression of SPARC in BC tissues was associated with poor patient survival (Figure 1H).

The epigenetic regulation mechanism of SPARC expression in BC. The CpG islands of SPARC were detected by MethPrimer and one CpG island was identified (Figure 2A). The expression levels of SPARC in six cell lines treated or untreated with 5-Aza-dC were measured by the qRT-PCR method, and the expression levels of SPARC were detected to be significantly increased in 5-Aza-dC treated MCF-10A, MCF-7, MDA-MB-549, and MDA-MB-231 cells, while significant variation was not detected in 5-Aza-dC treated MDA-MB-453 and SK-BR-3 cells (Figure 2B). Then, frequent hypermethylation of the CpG sites in the promoter and exon 1 regions of the SPARC gene was observed in MCF-10A, MCF-7, MDA-MB-453, and SK-BR-3 cells by BGS assay, especially in MCF-10A and MCF-7 cells (Figure 2C). According to the distribution of methylated CpG sites detected by BGS analysis, BS-MSP primers were designed. MCF-10A and MCF-7 cells showed fully methylation status before 5-Aza-dC treatment and the methylation status was completely reversed after 5-Aza-dC treatment. The MDA-MB-231 and BT-549 cells presented hemimethylation of SPARC before 5-Aza-dC treatment and demonstrated fully unmethylation status after 5-Aza-dC treatment. The methylation status of SPARC in MDA-MB-453 and SK-BR-3 cells showed no marked difference before and after 5-Aza-dC treatment (Figure 2D). The methylation status of SPARC was further detected by BS-MSP analysis in BC tissues and corresponding normal tissues (Figure 2E). The levels of promoter methylation of SPARC were somewhat different depending on the different molecular subtypes of BC (Figure 2F). Luminal A has the highest methylation levels while TNBC holds the lowest in the four BC subtypes. The methylation frequency of SPARC was associated with molecular subtype of BC and lymph node metastasis ($p<0.05$; Table 2). As expected, luminal A type demonstrated relatively high methylation levels while TNBC types showed the lowest methylation levels. Association between SPARC expression and methylation status was further analyzed by qRT-PCR. As demonstrated in Figure 2G, the mRNA expression levels of SPARC in methylated BC tissues were markedly decreased compared with unmethylated BC tissues. Moreover, mRNA expression levels of SPARC in unmethylated TNBC tissues were significantly higher than that in unmethylated luminal subtype tissues. The survival analysis revealed that hypomethylation of SPARC indicated a poor prognosis for BC patients (Figure 2H).

Table 1. Protein expression and methylation status of SPARC in BC tumor tissues and corresponding normal tissues.

Group	N	Protein expression		Methylation frequency	
		n (%)	p-value	n (%)	p-value
Normal tissues	120	18 (15.0)	0.001	92 (76.6)	0.001
Tumor tissues	120	42 (35.0)		67 (55.8)	

The functional analysis of overexpression SPARC in human breast cancer cell lines. As we have proved that MCF-7 cells demonstrated the lowest expression level of SPARC and hypermethylation status, while MDA-MB-231 cells showed the highest expression level of SPARC and hypomethylation, and MCF-7 cell is a luminal subtype cell line and MDA-MB-231 cell is a TNBC subtype cell line, thus we selected MCF-7 and MDA-MB-231 cells for the following gain- or loss-of-function experiments. The expression levels of SPARC were assessed in MCF-7 and MDA-MB-231 cells transfected with oeSPARC or oeNC by qRT-PCR and WB methods. The mRNA and protein expression levels of SPARC were significantly increased in oeSPARC transfected MCF-7 and MDA-MB-231 cells (Figure 3A). Overexpression of SPARC did not appreciably influence the proliferation of MCF-7 and MDA-MB-231 cells detected by CCK-8 and colony formation assays (Figures 3B, 3C). Overexpression of SPARC promoted the migration of MCF-7 and MDA-MB-231 cells detected by wound healing and Transwell migration assays (Figures 3D, 3E). Furthermore, overexpression of SPARC also increased the invasiveness of MCF-7 and MDA-MB-231 cells (Figure 3E).

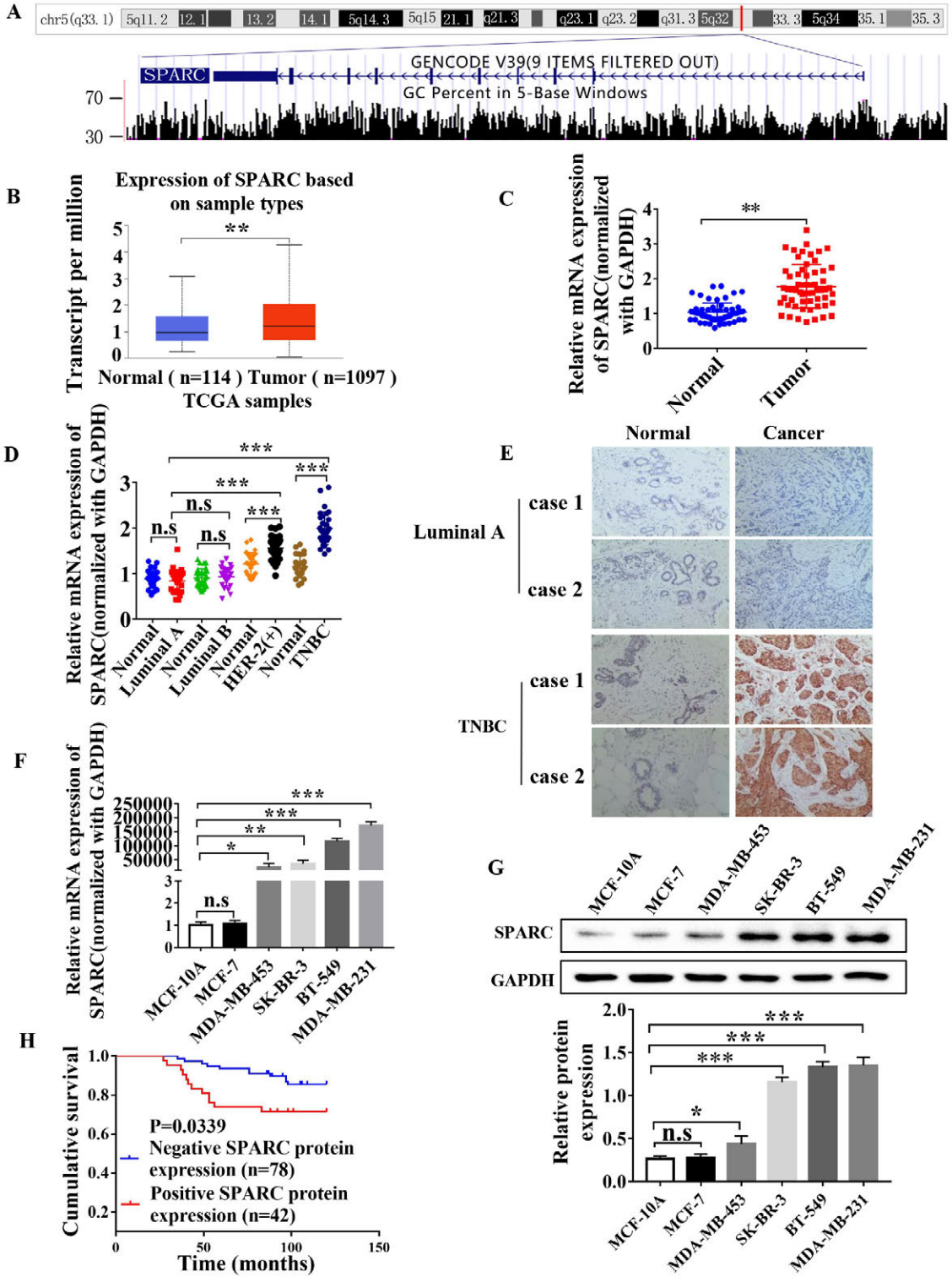

Figure 1. The expression status of SPARC in BC tissues and human breast cell lines. A) Schematic representation of the location of the SPARC gene and CpG sites distribution from the UCSC database. B) The mRNA expression levels of SPARC in breast cancer tissues and corresponding normal tissues were downloaded from TCGA database. The results are shown as ΔCt values normalized to GAPDH. C) The mRNA expression levels of SPARC in BC tissues and adjacent normal tissues. D) The mRNA expression levels of SPARC in tissues with different molecular subtypes of BC. E) The protein expression of SPARC was detected by immunohistochemical staining in BC tissues and adjacent normal tissues. F) The mRNA expression of SPARC in 6 cell lines. G) The protein expression of SPARC in 6 cell lines, and WB images of 6 cell lines were analyzed by ImageJ Software and quantified the gray scale values. H) Showing a direct correlation between positive SPARC protein expression and poor patient survival. *p<0.05, **p<0.01, ***p<0.001.

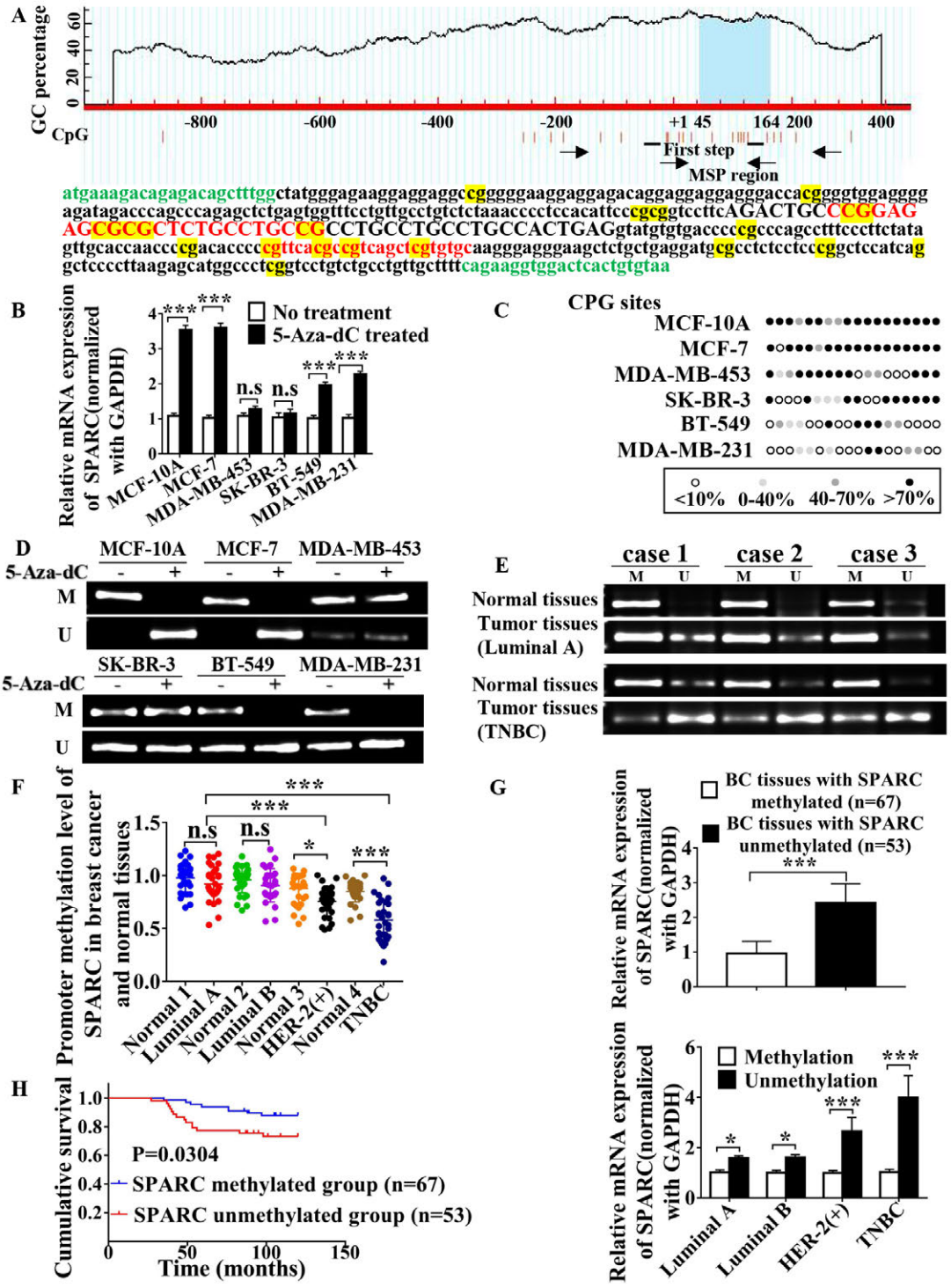

Figure 2. The epigenetic regulation of SPARC transcription in BC cell lines and BC tissues. A) Schematic structure of CpG islands in SPARC predicted by MethPrimer. The BGS and BS-MSP region analyzed was indicated. B) The mRNA expression of SPARC in 6 cell lines treated or untreated with 5-Aza-dC. C) Methylation status of each CpG site in the SPARC promoter region detected by BGS in 6 cell lines. Each CpG site was presented at the top row as an individual number. Methylation percentage was determined as a percentage of methylated cytosines from 10 sequenced colonies. The color of circles for each CpG site represented the percentage of methylation. D) Methylation status of SPARC was detected by bisulfite conversion-specific MSP in 6 cell lines. M, methylated; U, unmethylated. E) Methylation status of SPARC was detected by bisulfite conversion-specific MSP in luminal A and TNBC tissues. F) The levels of promoter methylation of SPARC in BC tissues with different molecular subtypes. G) The mRNA expression of SPARC in the tumor tissues with or without methylation of SPARC. The mRNA expression of SPARC in different molecular subtypes with or without SPARC methylation. H) Showing a direct correlation between SPARC unmethylated group and poor patient survival. *p<0.05, **p<0.01, ***p<0.001.

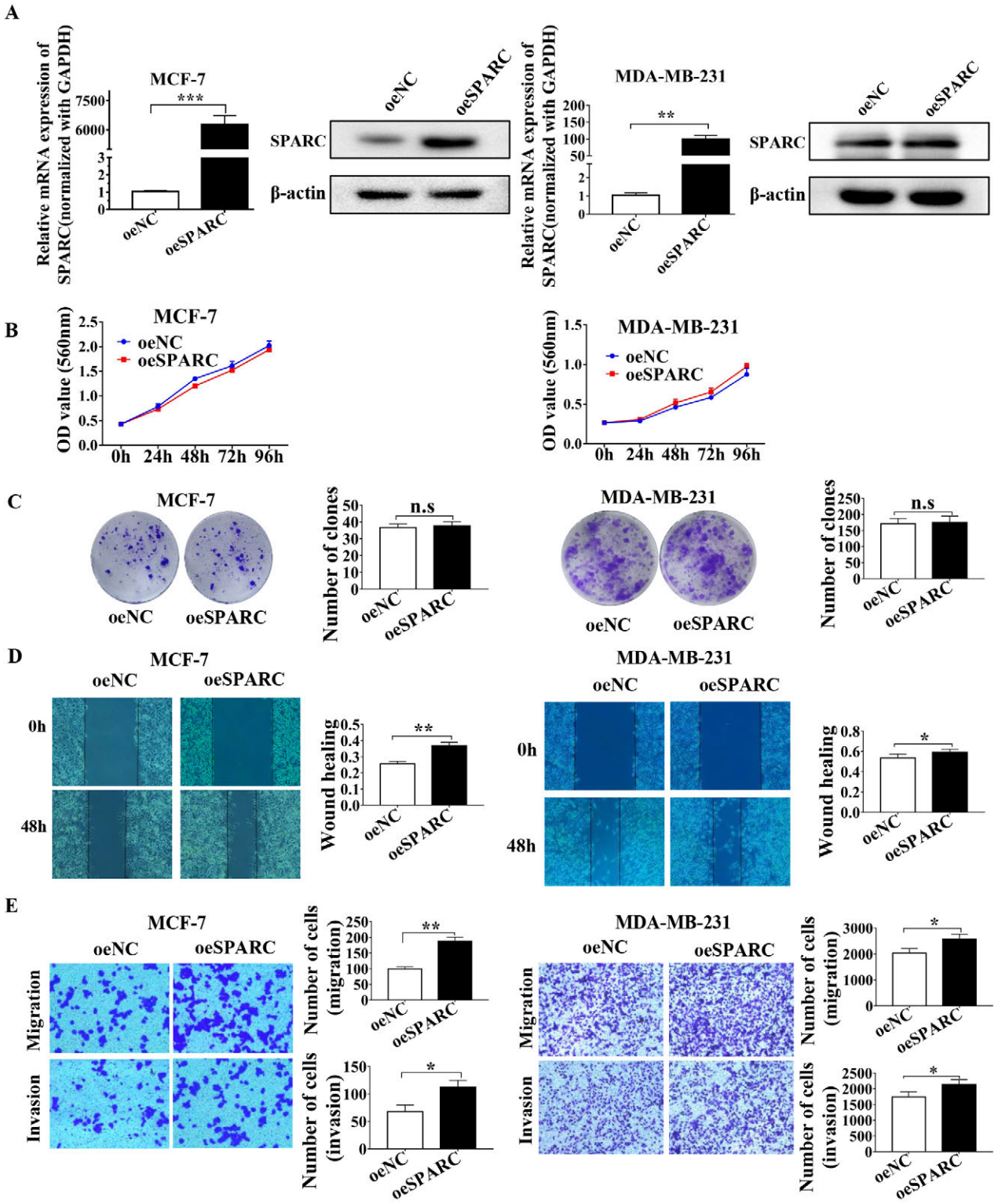

Figure 3. The functional analysis of overexpression SPARC in human breast cancer cell lines. A) The expression of SPARC in MCF-7 and MDA-MB-231 cells after transfection with oeSPARC was detected by qRT-PCR and WB methods. B) The proliferation of MCF-7 and MDA-MB-231 cells transfected with oeSPARC was detected by CCK-8 assay. C) Colony formation assay was used to determine the proliferation of MCF-7 and MDA-MB-231 cells transfected with oeSPARC. D) Wound healing assay was employed to detect the migration of MCF-7 and MDA-MB-231 cells transfected with oeSPARC. E) Transwell migration and Matrigel invasion assays were used to detect the migration and invasion ability of MDA-MB-231 and MCF-7 cells transfected with oeSPARC. *p<0.05, **p<0.01, ***p<0.001.

The functional analysis of knocking down SPARC in human breast cancer cell lines. The expression level of SPARC was detected in siSPARC-1/2 transfected MCF-7 and MDA-MB-231 cells by qRT-PCR and WB methods. The mRNA and protein expression levels of SPARC were significantly decreased in siSPARC-1/2 transfected MCF-7 and MDA-MB-231 cells (Figure 4A). Knockdown of SPARC could not obviously influence the proliferation of MCF-7 and MDA-MB-231 cells detected by CCK-8 and colony formation assays (Figures 4B, 4C). Knockdown of SPARC markedly inhibited migration and invasion of MDA-MB-231 cells detected by wound healing and Transwell assays (Figures 4D, 4E). While knockdown of SPARC expression did not appreciably affect MCF-7 cells' migration and invasion ability (Figures 4D, 4E).

Association between SPARC and EMT process in BC. Considering that overexpression or inhibition of SPARC could influence the migration and invasion capability of BC cells, we speculated that SPARC might participate in the EMT process, which is closely related to tumor invasion and metastasis. The expression levels of EMT-related genes were subsequently examined in SPARC overexpressed or knocked down cells. The mRNA expression levels of mesenchymal markers, N-cadherin, Vimentin, and β-catenin were found to be remarkably upregulated in SPARC overexpressed MCF-7 cells, while epithelial marker, E-cadherin was downregulated in SPARC overexpressed MCF-7 cells (Figure 5A). However, no changes in mRNA expression levels of EMT-related genes were found in SPARC overexpressed MDA-MB-231 cells (Figure 5A). The protein expression levels of EMT-related genes were also detected in SPARC overexpressed MCF-7 and MDA-MB-231 cells, and a similar expression trend as mRNA expression was found (Figure 5B). We further detected the expression level of EMT-related genes in SPARC knocked down MCF-7 and MDA-MB-231 cells. As shown in Figure 5C, the mRNA expression levels of E-cadherin were upregulated, while N-cadherin, Vimentin, and β-catenin were downregulated in siSPARC-1/2 transfected MDA-MB-231 cells. However, the expression changes were not found in siSPARC-1/2 transfected MCF-7 cells. Furthermore, a similar protein expression trend as mRNA expression of EMT-related genes was found in siSPARC-1/2 transfected MCF-7 and MDA-MB-231 cells (Figure 5D).

Table 2. Protein expression and methylation status of SPARC in tumor tissues.

Groups	N	Protein expression		Methylation frequency	
		n (%)	p-value	n (%)	p-value
Age					
<40	23	8 (34.7)	1.0	11 (47.8)	0.531
≥40	97	34 (35.1)		56 (57.7)	
Tumor diameter					
≤2 cm	96	33 (34.4)	0.962	55 (57.3)	0.679
>2 cm	24	9 (37.5)		12 (50.0)	
TNM stage					
I	8	3 (37.5)	0.878	5 (62.5)	0.918
II	89	30 (33.7)		49 (55.1)	
III	23	9 (39.1)		13 (56.5)	
Vascular tumor thrombus					
Positive	22	9 (40.9)	0.692	10 (45.4)	0.397
Negative	98	33 (33.6)		57 (58.1)	
Pathological type					
Ductal	107	38 (35.5)	0.975	58 (54.2)	0.463
Lobular	13	4 (30.7)		9 (69.2)	
Histological grade					
I grade	11	4 (36.4)	0.937	7 (63.6)	0.378
II grade	88	30 (34.1)		51 (58.0)	
III grade	21	8 (38.1)		9 (42.9)	
Molecular typing					
Luminal A	30	6 (20.0)	0.023	22 (73.3)	0.006
Luminal B	30	7 (23.3)		21 (70.0)	
HER-2 (+)	30	14 (46.6)		13 (43.3)	
TNBC	30	15 (50.0)		11 (36.7)	
LN metastasis					
Negative (N0)	58	14 (24.1)	0.026	39 (67.2)	0.024
Positive (N1/2/3)	62	28 (45.1)		28 (45.2)	
Distant metastases					
Negative	113	37 (32.7)	0.037	65 (57.5)	0.134
Positive	7	5 (71.4)		2 (28.6)	

Abbreviations: TNM-tumor-node-metastasis; TNBC-triple-negative breast cancer; LN-lymph node

Discussion

SPARC is well known to be involved in multiple processes of human cancers [20, 21]. SPARC exerts a complex role in different human cancers including BC. Several studies have reported that SPARC promoted the invasiveness of melanoma cells [22], accelerated the EMT process of hepatocellular carcinoma cells [23], and boosted the migration of endometrial cancer cells [24]. The protein expression level of SPARC was upregulated in oral squamous cell carcinoma [25]. High expression of SPARC was identified as a poor prognostic factor in cases with locally advanced non-small cell lung cancer (NSCLC) treated with concurrent chemoradiotherapy [26]. However, SPARC was reported to act as a tumor suppressor to decrease the proliferation of prostate cancer cells [11]. There were also some results indicating that SPARC suppressed bladder carcinogenesis, progression, and metastasis and induced neuroblastoma apoptosis [27, 28]. Clinical data revealed that decreased stromal SPARC expression was associated with breast cancer to bone metastasis [29]. Gain- and loss-of-function studies revealed that SPARC inhibited the migration and invasion of breast cancer cells, and suppressed osteoclast activation in the breast cancer microenvironment [29]. On the contrary, SPARC can be a new biomarker helpful to identify more aggressive ductal carcinoma in situ (DCIS) and for the prediction of invasive

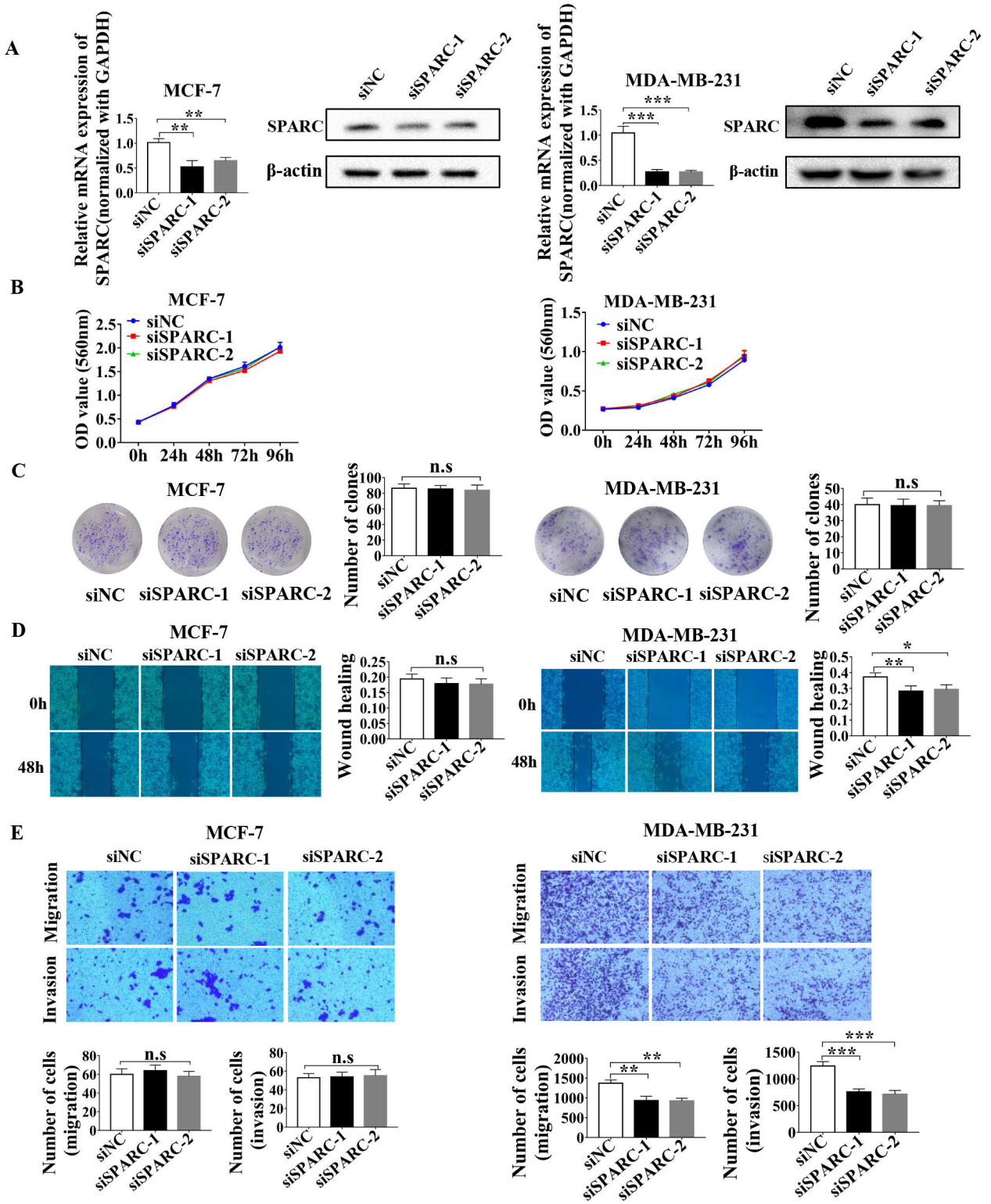

Figure 4. The functional analysis of silencing SPARC in human breast cancer cell lines. A) The expression of SPARC in MCF-7 and MDA-MB-231 cells after transfection with siSPARC was detected by qRT-PCR and WB methods. B) The proliferation of MCF-7 and MDA-MB-231 cells transfected with siSPARC was detected by CCK-8 assay. C) Colony formation assay was used to determine the proliferation of MCF-7 and MDA-MB-231 cells transfected with siSPARC. D) Wound healing assay was employed to detect the migration of MCF-7 and MDA-MB-231 cells transfected with siSPARC. E) Transwell migration and matrigel invasion assays were used to detect the migration and invasion ability of MDA-MB-231 and MCF-7 cells transfected with siSPARC. *p<0.05, **p<0.01, ***p<0.001.

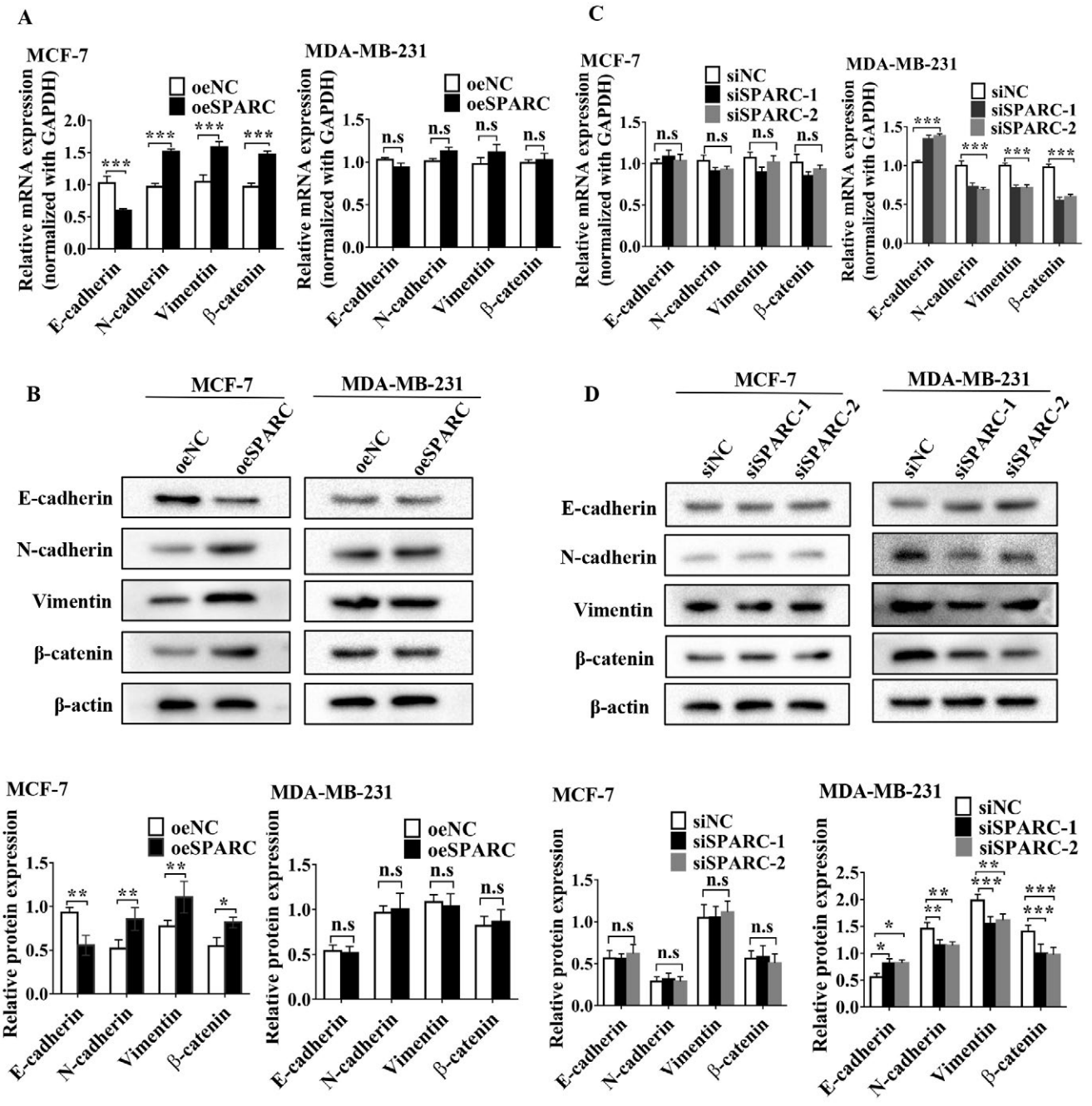

Figure 5. The confirmation of downstream genes and pathways in which SPARC was involved in. A, B) The mRNA and protein expression levels of E-cadherin, N-cadherin, Vimentin, and β-catenin in MCF-7 and MDA-MB-231 cells transfected with oeSPARC were analyzed by qRT-PCR and WB methods. C, D) The mRNA and protein expression levels of the selected differentially expressed genes in MCF-7 and MDA-MB-231 cells transfected with siSPARC were analyzed by qRT-PCR and WB methods. *p<0.05, **p<0.01, ***p<0.001.

disease on final pathology [14]. Another study implied that targeting SPARC expression by DNA methyltransferases blockade, and the combined treatment with miRNAs is a promising strategy to affect the invasive front of bone metastasis [30]. Over a 6-year follow-up verified that high levels of SPARC were associated with the overall survival of BC patients [31]. The detailed function of SPARC and its prognostic character in BC deserve to be further explored.

In the present study, remarkable upregulation of SPARC was detected in BC cell lines and BC samples, and the increased expression of SPARC in BC tissues was associated with molecular subtype and lymph node metastasis. There

were some papers reporting that expression of SPARC was associated with breast cancer cells growth and metastasis, more aggressive tumor types, and worse prognosis [32–35]. Recently, some clinical studies reported that analyses of molecular subtypes revealed an increased SPARC expression in patients with TNBC (37%) compared with HR (HR+/HER2– 23%) or HER2+ subtypes (HR+/HER2+ 29%; HR–/HER2+ 2%; $p = 0.037$). TNBC subtype is the most aggressive subtype of BC with a high probability of metastasis as well as a lack of specific targets and targeted therapeutics [36], while luminal BC represents the majority of breast cancer cases and with good prognosis [37]. These results were partially matched with our results. But they did not thoroughly explore the gain- and loss-of-function and molecular mechanism of SPARC in the progression of BC.

Promoter methylation of SPARC may be an important epigenetic mechanism involved in silencing its expression. Promoter methylation of SPARC was deeply investigated in ovarian cancer, colon cancers, and pancreatic adenocarcinoma, and promoter hypermethylation of SPARC was confirmed to result in the reduced expression [18, 38]. However, the promoter methylation status of SPARC in the pathogenesis of primary BC remains elusive. The mRNA and protein expression level of SPARC was significantly upregulated in most 5-Aza-dC-treated BC cells. However, there is no marking difference in the SPARC expression before and after 5-Aza-dC treatment in MDA-MB-453 and SK-BR-3 cells, the different molecular subtypes, and the using dose of 5-Aza-dC of the cell lines may be associated with the different sensitivity to 5-Aza-dC treatment. MCF-7 cells and luminal BC have low expression and hypermethylation of SPARC, and MDA-MB-231 cells and TNBC hold high expression and hypomethylation of SPARC. Combined with clinical features of BC that luminal BC are sluggish to metastasis, while TNBC are vibrant to metastasis, we confirmed that methylation of SPARC was involved in the progression of BC. Survival analysis demonstrated that upregulation and hypomethylation of SPARC were associated with poor BC patients' survival. These results indicated that aberrant methylation mediated upregulation of SPARC may be involved in the progression of BC.

We further performed gain- and loss-of-function experiment in two cell lines, MCF-7 cells, characterized by low expression of SPARC and almost without metastasis, and MDA-MB-231 cells with a peculiarity of high expression of SPARC and easily to metastasis. The results indicated that overexpression of SPARC dramatically promoted MCF-7 and MDA-MB-231 cells migration and invasion, while knockdown of SPARC inhibited migration and invasion of both cell lines. Essentially, MCF-7 cells showed a lower expression of SPARC ($\Delta Ct=18$, normalized to GAPDH) compared with MDA-MB-231 cells ($\Delta Ct=1$, normalized to GAPDH), which resulted that MCF-7 cells being easily to be overexpressed and showing more significant superiority in gain-of-function experiments with SPARC overexpression, in contrast, MDA-MB-231 cells were liable to be knocked down and showed a more significant preponderance in loss-of-function experiments with SPARC knockdown.

SPARC was previously reported to act as a tumor suppressor or tumor promoter to be involved in the proliferation of the prostate and hepatocellular cancer cells [39], however, few studies reported that SPARC was involved in the proliferation of breast cancer cells. Considering that overexpression or inhibition of SPARC could influence the migration and invasion capability of BC cells, we speculated that SPARC might participate in the EMT process in BC progression. We detected expression changes of E-cadherin, N-cadherin, Vimentin, and β-catenin in SPARC overexpressed and knockdown MCF-7 and MDA-MB-231 cells, suggesting that SPARC may participate in BC progression by influencing the EMT process. However, the specific mechanisms need to be further studied.

In summary, we showed for the first time that the expression levels of SPARC were regulated by promoter methylation status, and the high SPARC expression was significantly associated with unfavorable outcomes in BC. Upregulation of SPARC could facilitate BC development *in vitro*. SPARC might be identified as a potential prognostic indicator and therapeutic target for BC treatment.

Supplementary information is available in the online version of the paper.

References

[1] LI W, SANG M, HAO X, JIA L, WANG Y et al. Gene expression and DNA methylation analyses suggest that immune process-related ADCY6 is a prognostic factor of luminal-like breast cancer. J Cell Biochem 2020; 121: 3537–3546. https://doi.org/10.1002/jcb.29633

[2] SUNG H, FERLAY J, SIEGEL RL, LAVERSANNE M, SOERJOMATARAM I et al. Global Cancer Statistics 2020: GLOBOCAN Estimates of Incidence and Mortality Worldwide for 36 Cancers in 185 Countries. CA Cancer J Clin 2021; 71: 209–249. doi:10.3322/caac.21660

[3] LINDNER JL, LOIBL S, DENKERT C, ATASEVEN B, FASCHING PA et al. Expression of secreted protein acidic and rich in cysteine (SPARC) in breast cancer and response to neoadjuvant chemotherapy. Ann Oncol 2015; 26: 95–100. https://doi.org/10.1093/annonc/mdu487

[4] IKUTA Y, HAYASHIDA Y, HIRATA S, IRIE A, SENJU S et al. Identification of the H2-Kd-restricted cytotoxic T lymphocyte epitopes of a tumor-associated antigen, SPARC, which can stimulate antitumor immunity without causing autoimmune disease in mice. Cancer Sci 2009; 100: 132–137. https://doi.org/10.1111/j.1349-7006.2008.01016.x

[5] KIM NI, KIM GE, LEE JS, PARK MH. In phyllodes tumors of the breast expression of SPARC (osteonectin/BM40) mRNA by in situ hybridization correlates with protein expression by immunohistochemistry and is associated with tumor progression. Virchows Arch 2017; 470: 91–98. https://doi.org/10.1007/s00428-016-2048-0

[6] KUNIGAL S, GONDI CS, GUJRATI M, LAKKA SS, DINH DH et al. SPARC-induced migration of glioblastoma cell lines via uPA-uPAR signaling and activation of small GTPase RhoA. Int J Oncol 2006; 29: 1349–1357. https://doi.org/10.3892/ijo.29.6.1349

[7] VAJKOCZY P, MENGER MD, GOLDBRUNNER R, GE S, FONG TA et al. Targeting angiogenesis inhibits tumor infiltration and expression of the pro-invasive protein SPARC. Int J Cancer 2000; 87: 261–268. https://doi.org/10.1002/1097-0215(20000715)87:2<261:aid-ijc18>3.0.co;2-6

[8] YOSHIMURA T, NAGAHARA M, KUO C, TURNER RR, SOON-SHIONG P et al. Lymphovascular invasion of colorectal cancer is correlated to SPARC expression in the tumor stromal microenvironment. Epigenetics 2011; 6: 1001–1011. https://doi.org/10.4161/epi.6.8.16063

[9] CHANG CH, YEN MC, LIAO SH, HSU YL, LAI CS et al. Secreted Protein Acidic and Rich in Cysteine (SPARC) Enhances Cell Proliferation, Migration, and Epithelial Mesenchymal Transition, and SPARC Expression is Associated with Tumor Grade in Head and Neck Cancer. Int J Mol Sci 2017; 18: 1556. https://doi.org/10.3390/ijms18071556

[10] SATO N, FUKUSHIMA N, MAEHARA N, MATSUBAYASHI H, KOOPMANN J et al. SPARC/osteonectin is a frequent target for aberrant methylation in pancreatic adenocarcinoma and a mediator of tumor-stromal interactions. Oncogene 2003; 22: 5021–5030. https://doi.org/10.1038/sj.onc.1206807

[11] SHIN M, MIZOKAMI A, KIM J, OFUDE M, KONAKA H et al. Exogenous SPARC suppresses proliferation and migration of prostate cancer by interacting with integrin β1. Prostate 2013; 73: 1159–1170. https://doi.org/10.1002/pros.22664

[12] YIU GK, CHAN WY, NG SW, CHAN PS, CHEUNG KK et al. SPARC (secreted protein acidic and rich in cysteine) induces apoptosis in ovarian cancer cells. Am J Pathol 2001; 159: 609–622. https://doi.org/10.1016/S0002-9440(10)61732-4

[13] GILLES C, BASSUK JA, PULYAEVA H, SAGE EH, FOIDART JM et al. SPARC/osteonectin induces matrix metalloproteinase 2 activation in human breast cancer cell lines. Cancer Res 1998; 58: 5529–5536.

[14] SZYNGLAREWICZ B, KASPRZAK P, DONIZY P, BIECEK P, HALON A et al. Ductal carcinoma in situ on stereotactic biopsy of suspicious breast microcalcifications: Expression of SPARC (Secreted Protein, Acidic and Rich in Cysteine) can predict postoperative invasion. J Surg Oncol 2016; 114: 548–556. https://doi.org/10.1002/jso.24373

[15] KOBLINSKI JE, KAPLAN-SINGER BR, VANOSDOL SJ, WU M, ENGBRING JA et al. Endogenous osteonectin/SPARC/BM-40 expression inhibits MDA-MB-231 breast cancer cell metastasis. Cancer Res 2005; 65: 7370–7377. https://doi.org/10.1158/0008-5472.CAN-05-0807

[16] NAGARAJU GP, EL-RAYES BF. SPARC and DNA methylation: possible diagnostic and therapeutic implications in gastrointestinal cancers. Cancer Lett 2013; 328: 10–17. https://doi.org/10.1016/j.canlet.2012.08.028

[17] WENG JY, SALAZAR N. DNA Methylation Analysis Identifies Patterns in Progressive Glioma Grades to Predict Patient Survival. Int J Mol Sci 2021; 22: 1020. https://doi.org/10.3390/ijms22031020

[18] SOCHA MJ, SAID N, DAI Y, KWONG J, RAMALINGAM P et al. Aberrant promoter methylation of SPARC in ovarian cancer. Neoplasia 2009; 11: 126–135. https://doi.org/10.1593/neo.81146

[19] ENNOUR-IDRISSI K, DRAGIC D, DUROCHER F, DIORIO C. Epigenome-wide DNA methylation and risk of breast cancer: a systematic review. BMC Cancer 2020; 20: 1048. https://doi.org/10.1186/s12885-020-07543-4

[20] AHIR BK, ELIAS NM, LAKKA SS. SPARC overexpression alters microRNA expression profiles involved in tumor progression. Genes Cancer 2017; 8: 453–471. https://doi.org/10.18632/genesandcancer.130

[21] CHLENSKI A, LIU S, GUERRERO LJ, YANG Q, TIAN Y et al. SPARC expression is associated with impaired tumor growth, inhibited angiogenesis and changes in the extracellular matrix. Int J Cancer 2006; 118: 310–316. https://doi.org/10.1002/ijc.21357

[22] GIROTTI MR, FERNÁNDEZ M, LÓPEZ JA, CAMAFEITA E, FERNÁNDEZ EA et al. SPARC promotes cathepsin B-mediated melanoma invasiveness through a collagen I/α2β1 integrin axis. J Invest Dermatol 2011; 131: 2438–2447. https://doi.org/10.1038/jid.2011.239

[23] JIANG X, LIU F, WANG Y, GAO J. Secreted protein acidic and rich in cysteine promotes epithelial-mesenchymal transition of hepatocellular carcinoma cells and acquisition of cancerstem cell phenotypes. J Gastroenterol Hepatol 2019; 34: 1860–1868. https://doi.org/10.1111/jgh.14692

[24] YUSUF N, INAGAKI T, KUSUNOKI S, OKABE H, YAMADA I et al. SPARC was overexpressed in human endometrial cancer stem-like cells and promoted migration activity. Gynecol Oncol 2014; 134: 356–363. https://doi.org/10.1016/j.ygyno.2014.04.009

[25] JING Y, JIN Y, WANG Y, CHEN S, ZHANG X et al. SPARC promotes the proliferation and metastasis of oral squamous cell carcinoma by PI3K/AKT/PDGFB/PDGFRβ axis. J Cell Physiol 2019; 234: 15581–15593. https://doi.org/10.1002/jcp.28205

[26] KURTUL N, EROGLU C, UNAL D, TASDEMIR EA, ORHAN O et al. Prognostic value of SPARC expression in unresectable NSCLC treated with concurrent chemoradiotherapy. Asian Pac J Cancer Prev 2014; 15: 8911–8916. https://doi.org/10.7314/apjcp.2014.15.20.8911

[27] SAID N, FRIERSON HF, SANCHEZ-CARBAYO M, BREKKEN RA, THEODORESCU D. Loss of SPARC in bladder cancer enhances carcinogenesis and progression. J Clin Invest 2013; 123: 751–766. https://doi.org/10.1172/JCI64782

[28] SAILAJA GS, BHOOPATHI P, GORANTLA B, CHETTY C, GOGINENI VR et al. The secreted protein acidic and rich in cysteine (SPARC) induces endoplasmic reticulum stress leading to autophagy-mediated apoptosis in neuroblastoma. Int J Oncol 2013; 42: 188–196. https://doi.org/10.3892/ijo.2012.1678

[29] MA J, GAO S, XIE X, SUN E, ZHANG M et al. SPARC inhibits breast cancer bone metastasis and may be a clinical therapeutic target. Oncol Lett 2017; 14: 5876–5882. https://doi.org/10.3892/ol.2017.6925

[30] MATTEUCCI E, MARONI P, DISANZA A, BENDINELLI P, DESIDERIO MA. Coordinate regulation of microenvironmental stimuli and role of methylation in bone metastasis from breast carcinoma. Biochim Biophys Acta 2016; 1863: 64–76. https://doi.org/10.1016/j.bbamcr.2015.10.010

[31] WATKINS G, DOUGLAS-JONES A, BRYCE R, MANSEL RE, JIANG WG. Increased levels of SPARC (osteonectin) in human breast cancer tissues and its association with clinical outcomes. Prostaglandins Leukot Essent Fatty Acids 2005; 72: 267–272. https://doi.org/10.1016/j.plefa.2004.12.003

[32] JONES C, MACKAY A, GRIGORIADIS A, COSSU A, REIS-FILHO JS et al. Expression profiling of purified normal human luminal and myoepithelial breast cells: identification of novel prognostic markers for breast cancer. Cancer Res 2004; 64: 3037–3045. https://doi.org/10.1158/0008-5472

[33] HELLEMAN J, JANSEN MP, RUIGROK-RITSTIER K, VAN STAVEREN IL, LOOK MP et al. Association of an extracellular matrix gene cluster with breast cancer prognosis and endocrine therapy response. Clin Cancer Res 2008; 14: 5555–5564. https://doi.org/10.1158/1078-0432.CCR-08-0555

[34] GRAHAM JD, BALLEINE RL, MILLIKEN JS, BILOUS AM, CLARKE CL. Expression of osteonectin mRNA in human breast tumours is inversely correlated with oestrogen receptor content. Eur J Cancer 1997; 33: 1654–1660. https://doi.org/10.1016/s0959-8049(97)00182-2

[35] LAKHANI SR, REIS-FILHO JS, FULFORD L, PENAULT-LLORCA F, VAN DER VIJVER M et al. Prediction of BRCA1 status in patients with breast cancer using estrogen receptor and basal phenotype. Clin Cancer Res 2005; 11: 5175–5180. https://doi.org/10.1158/1078-0432.CCR-04-2424

[36] DEEPAK KGK, VEMPATI R, NAGARAJU GP, DASARI VR, NAGINI S et al. Tumor microenvironment: Challenges and opportunities in targeting metastasis of triple negative breast cancer. Pharmacol Res 2020; 153: 104683. https://doi.org/10.1016/j.phrs.2020.104683

[37] TABOR S, SZOSTAKOWSKA-RODZOS M, FABISIEWICZ A, GRZYBOWSKA EA. How to Predict Metastasis in Luminal Breast Cancer? Current Solutions and Future Prospects. Int J Mol Sci 2020; 21: 8415. https://doi.org/10.3390/ijms21218415

[38] YANG E, KANG HJ, KOH KH, RHEE H, KIM NK et al. Frequent inactivation of SPARC by promoter hypermethylation in colon cancers. Int J Cancer 2007; 121: 567–575. https://doi.org/10.1002/ijc.22706

[39] LIU Y, FENG Y, WANG X, YANG X, HU Y et al. SPARC Negatively Correlates With Prognosis After Transarterial Chemoembolization and Facilitates Proliferation and Metastasis of Hepatocellular Carcinoma via ERK/MMP Signaling Pathways. Front Oncol 2020; 10: 813. https://doi.org/10.3389/fonc.2020.00813

https://doi.org/10.4149/neo_2022_211002N1401

Methylation-mediated expression of SPARC is correlated with tumor progression and poor prognosis of breast cancer

Xiao-Long LI[1,2], Jia-Li LI[3], Dong-Jie QIU[4], Li MA[1,*]

Supplementary Information

Supplementary Table S1. Primer sequences, annealing temperature, and product size of SPARC and EMT related genes.

Gene	Primer sequence (5'-3')	Annealing temperature, °C	Product size, bp
SPARC	F: 5'-TGAGGTATCTGTGGGAGCTAATC-3'	57	128
	R: 5'-CCTTGCCGTGTTTGCAGTG-3'		
E-cadherin	F: 5'-CGGACGATGATGTGAACACC-3'	56	211
	R: 5'-TTGCTGTTGTGCTTAACCCC-3'		
N-cadherin	F: 5'-GAAAGACCCATCCACG-3'	52	224
	R: 5'-CCTGCTCACCACCACTA-3'		
Vimentin	F: 5'-GAGTCCACTGAGTACCGGAG-3'	57	192
	R: 5'-ACGAGCCATTTCCTCCTTCA-3'		
β-catenin	F: 5'-AAATTCTTGGCTATTACGACA-3'	52	166
	R: 5'-GCACCTTCAGCACTCT-3'		
GAPDH	F: 5'-AGGTGAAGGTCGGAGTCAACG-3'	56	104
	R: 5'-AGGGGTCATTGATGGCAACA-3'		

Abbreviations: SPARC-secreted protein acidic and rich in cysteine; GAPDH-glyceraldehyde-3phosphate dehydrogenase

Supplementary Table S2. Primer sequences and reaction conditions of SPARC.

Types	Gene	Primer sequence (5'-3')	Annealing temperature, °C	Product size, bp
BGS	SPARC	F: 5'-ATGAAAGACAGAGACAGCTTTGG-3'	53	418
		R: 5'-TTACACAGTGAGTCCACCTTCTG-3'		
BS-MSP	Methylation	F: 5'-TCGGAGAGCGCGTTTTGTTTGTCG-3'	60	126
		R: 5'-ACACACGAACTAACGACGTAAACG-3'		
	Unmethylation	F: 5'-TTGGAGAGTGTGTTTTGTTTGTTG-3'	52	126
		R: 5'-ACACACAAACTAACAACATAAACA-3'		

Abbreviations: BGS-bisulfite genomic sequencing; BS-MSP-bisulfite conversion-specific and methylation-specific polymerase chain reaction